

Article

PIRT the TRP Channel Regulating Protein Binds Calmodulin and Cholesterol-Like Ligands

Nicholas J. Sisco ^{1,2,†} , Dustin D. Luu ^{1,2,†}, Minjoo Kim ^{1,2} and Wade D. Van Horn ^{1,2,*} 

¹ The School of Molecular Sciences, Arizona State University, Tempe, AZ 85287, USA; njsisco@asu.edu (N.J.S.); ddllu@asu.edu (D.D.L.); mkim89@asu.edu (M.K.)

² The Virginia G. Piper Biodesign Center for Personalized Diagnostics, Biodesign Institute, Arizona State University, Tempe, AZ 85281, USA

* Correspondence: wade.van.horn@asu.edu; Tel.: +1-(480)-965-8322; Fax: +1-(480)-965-2747

† These authors contributed equally to this work.

Received: 1 February 2020; Accepted: 17 March 2020; Published: 21 March 2020



Abstract: Transient receptor potential (TRP) ion channels are polymodal receptors that have been implicated in a variety of pathophysiologicals, including pain, obesity, and cancer. The capsaicin and heat sensor TRPV1, and the menthol and cold sensor TRPM8, have been shown to be modulated by the membrane protein PIRT (Phosphoinositide-interacting regulator of TRP). The emerging mechanism of PIRT-dependent TRPM8 regulation involves a competitive interaction between PIRT and TRPM8 for the activating phosphatidylinositol 4,5-bisphosphate (PIP₂) lipid. As many PIP₂ modulated ion channels also interact with calmodulin, we investigated the possible interaction between PIRT and calmodulin. Using microscale thermophoresis (MST), we show that calmodulin binds to the PIRT C-terminal α -helix, which we corroborate with a pull-down experiment, nuclear magnetic resonance-detected binding study, and Rosetta-based computational studies. Furthermore, we identify a cholesterol-recognition amino acid consensus (CRAC) domain in the outer leaflet of the first transmembrane helix of PIRT, and with MST, show that PIRT specifically binds to a number of cholesterol-derivatives. Additional studies identified that PIRT binds to cholecalciferol and oxytocin, which has mechanistic implications for the role of PIRT regulation of additional ion channels. This is the first study to show that PIRT specifically binds to a variety of ligands beyond TRP channels and PIP₂.

Keywords: PIRT; TRP channels; PIP₂; calmodulin; β -estradiol; nuclear magnetic resonance; microscale thermophoresis

1. Introduction

Transient receptor potential (TRP) ion channels respond to a variety of stimuli with pathophysiological implications in pain, obesity, and cancer [1–6]. TRPV1 is activated by heat, protons, and capsaicin, which is a pungent vanilloid compound [7,8]. TRPV1 function is further modulated by calcium [9], calmodulin (a calcium-binding protein) [10,11], PIP₂ [11], and a small membrane protein named PIRT (phosphoinositide interacting regulator of TRPs) [12–14]. Functionally opposite to TRPV1, TRPM8 is activated by cold, basic pH, and menthol. Like TRPV1, TRPM8 function is also modulated by calcium [15], calmodulin [11,16–21], PIP₂ [22], and PIRT [23,24]. PIRT modulation of these channels is the least well-characterized.

PIRT, Phosphoinositide-interacting regulator of TRP, was originally identified as a membrane protein that modulates TRP channel function and which binds phosphoinositides [9]. Additionally, it was shown to be expressed in the dorsal root ganglia and trigeminal ganglia of the peripheral nervous system, where, in mice, it enhances TRPV1-dependent currents [12]. More recently, PIRT was

shown to regulate TRPV1 with neuropathic pain implications [25], and TRPV1-dependent uterine contraction pain [14]. PIRT is also a regulatory subunit for TRPM8, where it displays species-dependent effects enhancing and attenuating TRPM8-dependent conductance in the rodent and human proteins, respectively [23]. PIRT regulation of TRPM8 appears to arise through competitively binding and modulating access of the lipid PIP₂ [22,23].

Despite a preponderance of data showing that PIRT regulates TRP channels, there is a growing body of evidence showing that PIRT has regulatory functions that may not be directly related to TRP channels. It has been reported to interact with P2 × 3 channels and that it could impact overactive bladder [26], and also co-localizes with P2X2 within the enteric nervous system [27]. Given that PIRT interacts with PIP₂, and that a number of PIP₂-dependent channels are also calmodulin-regulated [11,16,28–30], we sought to investigate if PIRT interacts with calmodulin and other common modalities that impact ion channel function.

The highly conserved calcium sensor, calmodulin (CaM), is a known ion channel regulator [17,19,31–33] that downregulates Ca²⁺-permeable cation channels, including TRP channels, through a negative feedback mechanism that prevents excessive calcium influx [1]. In TRPV1, CaM competes for a binding site with PIP₂ and another calcium-binding protein, S100A1 [11]. There is direct evidence that CaM binds to isolated TRPV1 peptides [10]. Complementing this evidence are cryo-EM structures of a related channel, TRPV6, which identifies the location and stoichiometry of the interaction [18]. The structure reveals that CaM binds to TRPV6 in a region that is structurally homologous to the bacterial potassium channel KCNQ1 [21]. It is plausible, based on a conserved CaM binding region in TRPV6, that TRPV1 and TRPM8 bind to CaM in an analogous manner.

TRPM8 is functionally modulated by CaM, where it desensitizes channel conductance in a PIP₂ dependent manner [16] with calcium influx leading to CaM and PIP₂-dependent desensitization of TRPM8. It is now understood that TRPM8 binds to and is regulated by both PIRT and PIP₂ [24,34]; however, it is not currently clear how the CaM-dependent modulatory process functions in the context of PIRT. Nonetheless, with the evidence that PIRT, TRPV1, and TRPM8 bind PIP₂ [11,12,22–24,35–38], and given the common interdependence of PIP₂–CaM regulation of ion channels, we hypothesize that PIRT may have a yet to be a determined role in CaM-dependent TRP channel regulation.

Herein, we predict a CaM binding site in the human PIRT using established bioinformatic techniques [39] and then use this information to guide binding assays to identify the amino acids that bind CaM. Our results show that PIRT and CaM bind to each other, which likely leads to the modulation of ion channel access to PIP₂ and calcium, both of which regulate TRPM8, TRPV1, and other channels with which PIRT may yet interact. Encouraged by the CaM binding data, we used additional bioinformatics tools and surveyed the literature to identify additional potential PIRT binding molecules. Using microscale thermophoresis (MST), our ligand screen focused on a number of cholesterol-like molecules, including cholesteryl-hemisuccinate, cortisol, and β-estradiol, and other TRP channel modulator ligands, including oxytocin and cholecalciferol, we show that the cholesterol-like compounds bind PIRT at a previously unrecognized cholesterol-binding domain (CRAC) [40] and that PIRT shows specificity for β-estradiol but not testosterone and for oxytocin over vasopressin. The ability of PIRT to bind these ligands suggests that it functions as a multimodal TRP channel modulator with implications in other ion channel functions.

2. Materials and Methods

2.1. Rosetta Flexible Peptide and High-Resolution Docking

We used Rosetta ab initio flexible peptide docking protocols [41] to fold and dock the PIRT C-terminal α-helix (residues 112–137) into the NMR structure of CaM (PDB: 2K0F). We generated 3, 5, and 9-mer fragments for PIRT according to established chemical shift quota filtered fragment generation protocols that are commonly used for Chemical-Shift-Rosetta (CS-Rosetta) [42]. We used these fragments and ensemble state number one from 2K0F to calculate 80,000 docking decoys. The

lowest scoring decoy was used to rescore the docked decoys, where the corresponding energy funnel signifies convergence. As per standard docking and Rosetta analysis protocols, we selected the decoy with the lowest interface score decoy with the lowest RMSD as the converged or working model to do a final standard fast relax [43].

2.2. Protein Expression and Purification

The expression and purification of PIRT were carried out following the established protocols in our previous work on PIRT [23,24].

Human CaM was expressed at 37 °C with a hexahistidine tag comprising MGHHHHHHG- inserted into a pET29 vector with kanamycin resistance and overexpressed in BL21 (DE3) cells. The cells were grown in ¹⁴N-M9 minimal media (42 mM disodium phosphate (Sigma-Aldrich), 17 mM dipotassium phosphate (Sigma-Aldrich), 8 mM sodium chloride (Sigma-Aldrich), 17 mM ammonium chloride (Sigma-Aldrich), 1× working solution of MEM vitamin solution (Corning), 1 mM magnesium sulfate (Sigma-Aldrich), 100 μM calcium chloride (Sigma-Aldrich), and 22 mM D-glucose (Sigma-Aldrich)). For NMR studies on ¹⁵N-calmodulin, ¹⁵N-ammonium chloride was the sole nitrogen source in the M9 minimal media. The cells were induced at OD₆₀₀ = 0.6 with 0.5 mM IPTG (Sigma-Aldrich). The cells were pelleted after 5 hr of induction at 6000×g at 4 °C for 20 min, which resulted in 3 g of cellular mass per 500 mL of M9 culture.

The cell pellet was resuspended and homogenized by tumbling for 1 hr in lysis buffer consisting of lysozyme (0.2 mg/mL), RNase (0.02 mg/mL), DNase (0.02 mg/mL), 1 mM phenylmethanesulfonylfluoride (PMSF, Sigma-Aldrich), 5 mM magnesium acetate (Sigma-Aldrich), 50 mM HEPES (Sigma-Aldrich) at pH 7.7, and 300 mM NaCl. The suspended cells were lysed using a sonicator (QSonica Q500) at 50% duty cycle and 50% amplitude for 7.5 min total on time. Cellular debris was removed with centrifugation of cell lysate at 38,000×g at 4 °C for 20 min. The supernatant was used for the following steps after discarding the pellet. The supernatant was tumbled for 1 hr and then loaded onto 2 mL of pre-equilibrated Ni-NTA (QIAGEN: 2 mL of resin per gram of cell pellet) within a gravity column. The Ni-NTA was pre-equilibrated with lysis buffer (50 mM HEPES (Sigma-Aldrich) pH 7.7 and 300 mM NaCl). Purification was then carried out with a flow-through buffer (50 mM HEPES pH 7.5), low imidazole wash (50 mM HEPES pH 7.5, 10 mM imidazole), and finally an elution buffer (50 mM HEPES pH 7.5, 300 mM imidazole). Following Ni-NTA chromatography, the eluent was concentrated to a volume of 500 μL and loaded directly onto a 60 mL column volume Superdex 200 (GE Healthcare Life Sciences) pre-equilibrated with 50 mM HEPES at pH 7.5 and separated by size. CaM purity was assessed with SDS-PAGE and the identity confirmed by western blot analysis with a penta-histidine primary antibody and anti-mouse alkaline phosphatase detection (Figure S1). We then used NMR to show that our CaM construct retains functional properties by heteronuclear single-quantum coherence (HSQC) NMR in the presence and absence of calcium. The resulting spectra show characteristic chemical shift perturbation for CaM (Figure S1).

For the pull-down experiment, the His-tagged CaM was buffer exchanged using a 10 kDa cutoff Amicon Ultra centrifugal filter (Millipore) into a thrombin cleavage buffer (25 mM Na₂HPO₄, 150 mM NaCl, pH 7.8) following Ni-NTA purification. The sample was then tumbled with 3 units of thrombin (Novagen) for 24 h at room temperature before flowing over Ni-NTA. The collected flow-through contained His-tag cleaved CaM, which was further purified by gel filtration chromatography.

2.3. Microscale Thermophoresis

Human PIRT was fluorescently labeled according to previous protocols [24]. For the MST measurements, the concentration of PIRT was kept consistent at 200 nM for all ligands in MST buffer (0.1% DPC (*w/v*), 50 mM HEPES, pH 7.0). Apo-CaM was purified as mentioned above, with 0.5 mM EDTA added to the size exclusion buffer and kept consistent throughout the MST measurements.

Cortisol, β-estradiol, testosterone, cholesteryl-hemisuccinate, and cholecalciferol were all solubilized as stock solutions in neat chloroform. From the ligand stock solutions, the desired

amount of the ligand for MST experiments was aliquoted into 200 μ L PCR tubes, and the chloroform was evaporated off under streaming N_2 at room temperature. The compounds were then resuspended in MST buffer with 200 nM PIRT. The disposal of testosterone was carried out according to U.S. Drug Enforcement Administration (DEA) standards under Title 21 Code of Federal Regulations. Oxytocin, vasopressin, calcium chloride, and nicotinamide stock solutions were prepared directly in MST buffer and aliquoted to desired concentrations for MST analysis.

The MST labeled PIRT was added to the solutions and incubated for 1 hr at room temperature. After incubation, a standard MST glass capillary tube (NanoTemper) was drawn into the tube by capillary action (~ 5 μ L). MST experiments were carried out in triplicate at room temperature with 50% infrared laser power and green channel using 10% excitation power.

All of the data from the MST ligand screen that showed ligand-dependent thermophoresis were normalized to free PIRT and bound PIRT following established protocols [44,45], from which the dissociation constant was calculated. Ligand-independent (i.e., non-binding) thermophoresis is evident in the controls (Figures S2A and S3). Ligand titration concentrations were optimized to show saturation and minima within the bounds of solubility; i.e., the cholesterol-like ligands tended to become insoluble above the concentrations used. The data were fit with in-house Python scripts where the errors are reported as the root-mean-square error (RMSE) of the fit. Typically, membrane protein binding studies of hydrophobic compounds use units of mole percent [24,44,46]. However, given that we screened both hydrophobic and hydrophilic compounds, we used molar-dependent units with a constant PIRT and membrane mimic concentration in order to compare the binding studies across chemical environments.

2.4. PIRT and Calmodulin Pull-Down Assay

The pull-down experiment was conducted by mixing 10 μ g His-tagged PIRT to 20 μ g CaM (sans His-tag) and tumbled at room temperature to allow the mixture to come to equilibrium. The sample was then exposed to 200 μ L of Ni^{2+} -bound nitrilotriacetic acid (Ni-NTA) resin and washed with 50 column volumes of 50 mM HEPES, 0.1% DDM, pH 7.5 to elute any unbound CaM. The bound sample was then eluted with 50 mM HEPES, 0.1% DDM, 500 mM imidazole, pH 7.5, and analyzed by SDS-PAGE gel.

2.5. Nuclear Magnetic Resonance-Detected Binding Assay

^{15}N -human PIRT (180 μ L, 3 mm NMR tube) and ^{15}N -human CaM (550 μ L, 5 mm NMR tube) were measured in NMR buffer (4% D_2O (v/v, Sigma Aldrich), 20 mM sodium phosphate (Fisher Scientific), 500 μ M DSS (Sodium trimethylsilylpropanesulfonate, Sigma Aldrich), and 0.5 mM EDTA (Sigma Aldrich) at pH 6.5) on a Bruker 850 MHz 1H magnet with Avance III console. Two thousand forty-eight direct points and 128 indirect points were collected with 128 transients, processed in NMRpipe [47], and analyzed in CCPNMR [48]. Optimization of NMR conditions for PIRT was carried out previously [24], resulting in dodecylphosphocholine (DPC) as the most suitable detergent for investigations with PIRT and at a temperature of 40 $^{\circ}C$. An HSQC of ^{15}N -human CaM was measured with and without $CaCl_2$ to show that it was properly folded in the conditions we tested.

To validate the cholesterol-like and β -estradiol binding site, a saturating concentration of β -estradiol (3.82 mole %) was dissolved in DMSO before adding to a ^{15}N -human PIRT sample. An HSQC of human PIRT was measured before and after adding β -estradiol, and the resonances with significant chemical shift perturbation identify the amino acids that comprise the binding site.

3. Results

3.1. Bioinformatic Analysis of PIRT Predicts Calmodulin-Binding Motifs

The CaM 1-14 motif has a consensus sequence of (FLIVW)- X_{12} -(FLIVW), where the X is any amino acid flanked by hydrophobic Phe, Leu, Ile, Val, or Trp. With the CaM target database web server [49], PIRT was identified to contain a highly conserved 1-14 calmodulin-binding motif in the C-terminal

still high with Arg121 to being overall highly conserved. We did not attempt to validate the predicted CaMKII motifs, but 185 mention them here for completeness.

3.2. Flex Pep Dock

Using Rosetta flexible peptide ab initio docking protocols, we were able to model how the positively charged C-terminal α -helix of PIRT might bind with the negatively charged calmodulin. We previously assigned the amino acid backbone resonances for the C-terminal amino acids from Lys117–Arg137 and used these assignments to make experimentally constrained fragments, which take into account the φ/ψ angles derived from NMR as well as evolutionarily conserved φ/ψ angles for stretches of similar amino acids. The Rosetta calculations show clear convergence (Figure S5) and localize the C-terminal α -helix to our predicted 1–14 CaM-binding motif (Figure 1A). The helical wheel representation (Figure 1B), made with using the European Molecular Biology Open Software Suite [51], shows that it is certainly possible for there to be two different 1–14 site that would be amenable for binding within the CaM hydrophobic pockets; however, our models predominately found the position Ile114 to Leu127 to be the lowest-scoring; i.e., lowest energy, and therefore, best docking (Figure S5).

3.3. PIRT Specifically Interacts with Calmodulin

PIRT has a high affinity for calcium-free CaM (apo-CaM) and a reduced affinity for calcium bound calmodulin. The MST binding screen shows that PIRT binds tightly in the mid to low nM range, $K_d = 350 \pm 40$ nM for apo-CaM (Table 1, Figure 2A). Calcium bound CaM (holo-CaM) has a decreased affinity for PIRT (i.e., weaker binding) and right-shifts the binding curve by about 200-fold to an apparent $K_d = 60 \pm 30$ μ M (Table 1, Figure 2A). PIRT does not bind to calcium chloride (Figures S2A and S3A).

Table 1. Ligands bound to PIRT using MST.

Ligand	K_d (M)	RMSE (M)	Ligand Type
Calmodulin (apo, free)	350×10^{-9}	40×10^{-9}	CaM, Intracellular Protein
Calmodulin (holo, bound)	60×10^{-6}	30×10^{-6}	Calcium Bound CaM
Cholesteryl HS	103×10^{-6}	6×10^{-6}	Steroid Hormone Precursor
Cortisol	790×10^{-6}	50×10^{-6}	Cortical Steroid Hormone
β -Estradiol	800×10^{-6}	100×10^{-6}	Sex Steroid Hormone
Cholecalciferol	2.1×10^{-3}	0.4×10^{-3}	Secosteroid Hormone
Oxytocin	7×10^{-6}	1×10^{-6}	Peptide Hormone

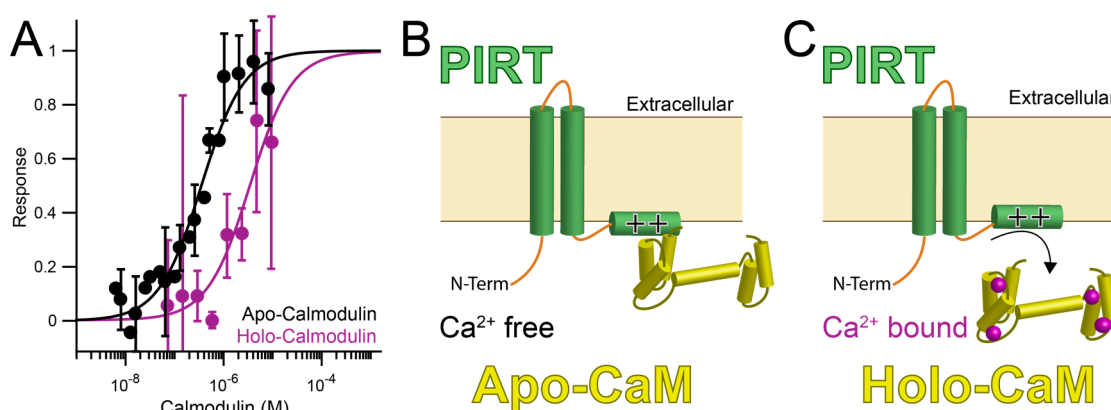


Figure 2. PIRT (Phosphoinositide-interacting regulator of TRP) binds to calcium-free calmodulin (apo-CaM) and calcium bound calmodulin (holo-CaM). (A) PIRT binds calcium-free calmodulin (apo-CaM, black) with approximately 200-fold higher affinity than Ca²⁺-bound calmodulin (holo-CaM, purple). (B) The differences in affinity suggest the possibility that PIRT is bound to apo-CaM until intracellular calcium levels rise high enough for holo-CaM to bind calcium and release PIRT (C).

To verify the CaM–PIRT interaction, a pull-down assay was conducted by mixing purified His-tagged PIRT with His-cleaved CaM at room temperature and then tumbled with Ni-NTA resin. The sample was washed extensively with 50 column volumes to remove any unbound protein. CaM co-elutes with the imidazole elution of PIRT. The Coomassie stain gel shows that PIRT and CaM were co-eluted confirming direct binding between PIRT and CaM (Figure S6).

3.4. NMR Titration Shows Residues with Ligand-Dependent Perturbation Including the Predicted Calmodulin Binding Site

NMR-detected ^{15}N labeled PIRT titrations with CaM show chemical shift perturbations for calcium-free CaM (Figure 3A) within the C-terminal α -helix (Figure 3B). Interestingly, Ser124 shows perturbations suggestive of slow-exchange on the NMR timescale with the disappearance of the initial peak, presumably the ligand-free state, and reappearance of the apparent bound peak across the titration concentrations; a hallmark of slow-exchange and tight binding. In addition to Ser124, chemical shift perturbation is also seen for His120 in the predicted 1–14 calmodulin-binding motif, while residues Lys131, Ser132, Leu135, and Arg137 also show chemical shift perturbation and are found in close proximity to the binding motif (Figure 1C).

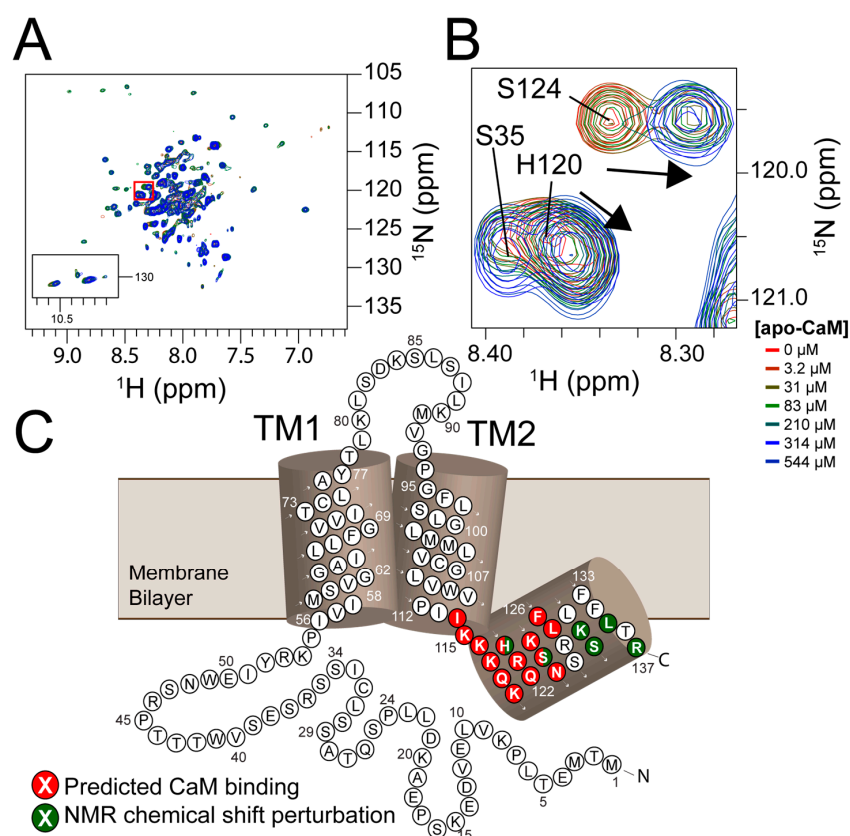


Figure 3. PIRT has residues that bind to calcium-free calmodulin in the C-terminal α -helix that is located in or near the 1-14 motif. (A) The HSQC follows the titration of NMR invisible ^{14}N -calcium-free calmodulin with NMR-detected ^{15}N -PIRT with concentrations of 0, 3.2, 31, 83, 210, 314, 544 μM calcium-free calmodulin. (B) Highlighted from the red inset on the HSQC are Ser35 showing no perturbation, His120 showing chemical shift perturbation show with the arrow, and Ser124 showing an apparent slow exchanging resonance with the arrow highlighting the movement. In (C), the calmodulin-binding motif is highlighted in red from Ile114 to Leu127 that was shown with Rosetta flexible docking to be the best fitting motif. Highlighted in dark green are residues that show chemical shift perturbations with the NMR titration.

3.5. Two Cholesterol-Binding Motifs Found on PIRT with Bioinformatic Analysis

PIRT has two putative cholesterol binding motifs in the first transmembrane α -helix. Cholesterol-binding proteins share a consensus sequence motif named cholesterol_recognition_amino_acid_consensus called CRAC, and CARC, where CARC is the mirror image of CRAC. The CRAC amino acid sequence is (L/V)-X₁₋₅-(Y)-X₁₋₅-(K/R), with N to C terminal directionality, and X stands for any amino acids [40]. Using the known molecular motifs for cholesterol-binding proteins, we report two cholesterol-like binding sites in the first transmembrane α -helix of human PIRT with CRAC in the outer leaflet of the membrane bilayers and CARC in the inner leaflet (Figure 4 and Figure S4).

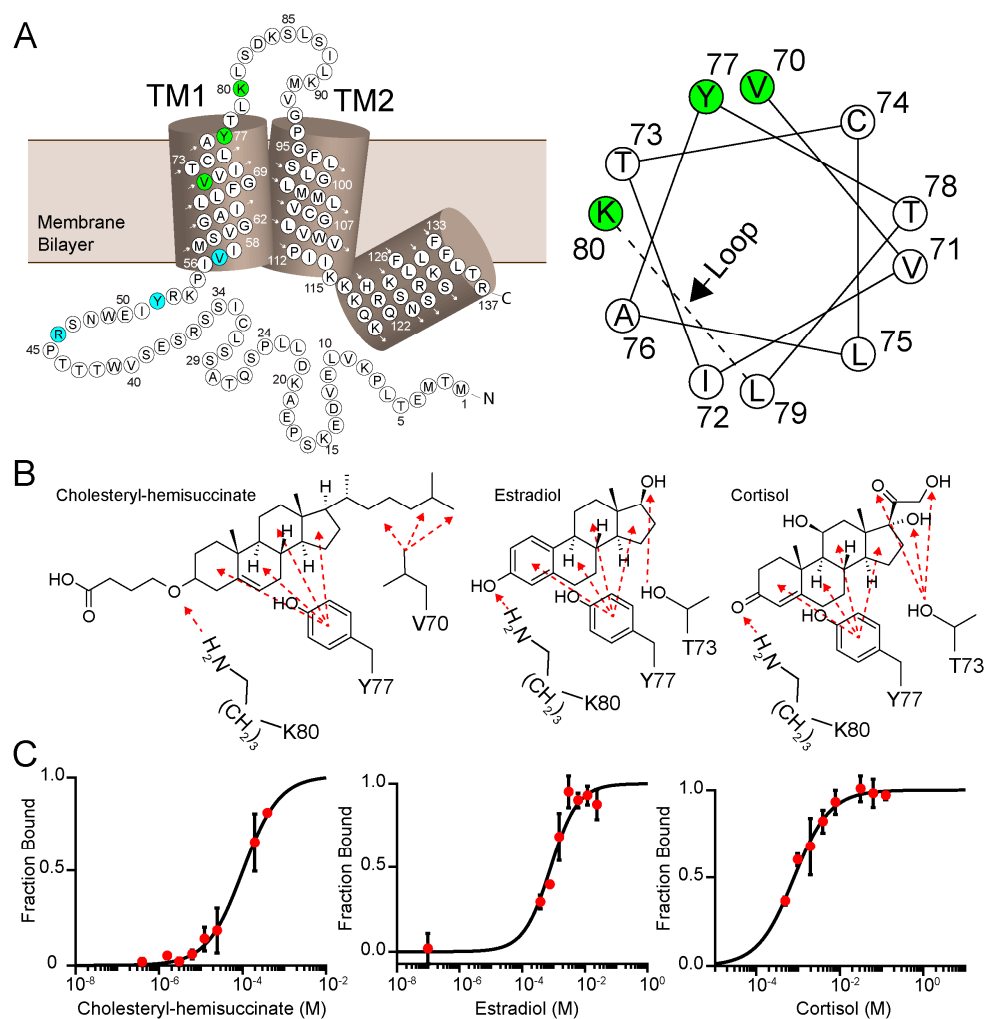


Figure 4. PIRT has a conserved cholesterol-binding CRAC and CARC motif. (A) We analyzed the PIRT sequence and identify that it contains a CRAC motif in the outer leaflet of the first transmembrane α -helix with amino acids highlighted in green and a CARC domain in the inner leaflet with amino acids highlighted in cyan. Shown in the helical wheel projection, the CRAC domain is supported with the evidence that within a standard α -helix, the Val70-Tyr77-Lys80 are on the same interface and are confirmed to bind to cholesterol with the NMR data below. (B) The amino acids that may bind to cholesterol hemisuccinate, β -estradiol, and cortisol and are shown here as an example of how PIRT could bind these ligands. To bind the β -estradiol or cortisol, we show here that PIRT could incorporate Thr73, which is on the same interface as the CRAC domain residues. In Figure S4, our alignment highlights a second cholesterol-binding domain, CARC, it resides outside of the membrane bilayer, does not have a helical interface consistent with a standard α -helix, and is not highlighted here. (C) PIRT ligand-dependent thermophoresis of cholesteryl-hemisuccinate, β -estradiol, and cortisol. The K_d values are listed in Table 1.

3.6. PIRT and Cholesterol Ligands Screening with Microscale Thermophoresis

We used microscale thermophoresis to investigate PIRT–cholesterol interactions. Given the solubility limitations of cholesterol, we tested the predicted cholesterol-binding with the more soluble cholesteryl-hemisuccinate, which shows an affinity of $103 \pm 6 \mu\text{M}$ (Figure 4). Cholesterol derivatives also bind PIRT with cortisol and β -estradiol K_d values of $790 \pm 60 \mu\text{M}$ and $800 \pm 100 \mu\text{M}$, respectively (Figure 4). Surprisingly, testosterone does not bind to PIRT (Figure S3B) despite its structural similarity to cholesterol, cortisol, and β -estradiol.

3.7. β -Estradiol Induced PIRT Chemical Shift Perturbation

To validate the predicted CRAC cholesterol-binding site in PIRT, a saturating concentration of β -estradiol was added to ^{15}N labeled PIRT. The resulting TROSY-HSQC spectra show chemical shift perturbations primarily in the upper transmembrane α -helix 1 (TM1) with a few that breach to the upper transmembrane α -helix 2 (TM2) (Figure 5). More specifically, chemical shift perturbations were seen at residues Ser60, Val61, Thr73, Tyr77, Lys80, and Leu81 in TM1 while Gly95 and Leu97 are seen in the TM2. The NMR data confirm the CRAC binding site location (Figures 4 and 5). The NMR data also show limited perturbation away from the CRAC site upon β -estradiol binding, with chemical shift perturbation of Ser60 and Val61 in TM1 and Gly95 and Leu97 in TM2, which are outside of the predicted CRAC domain, this could indicate that β -estradiol induces a change in PIRT conformation or dynamics.

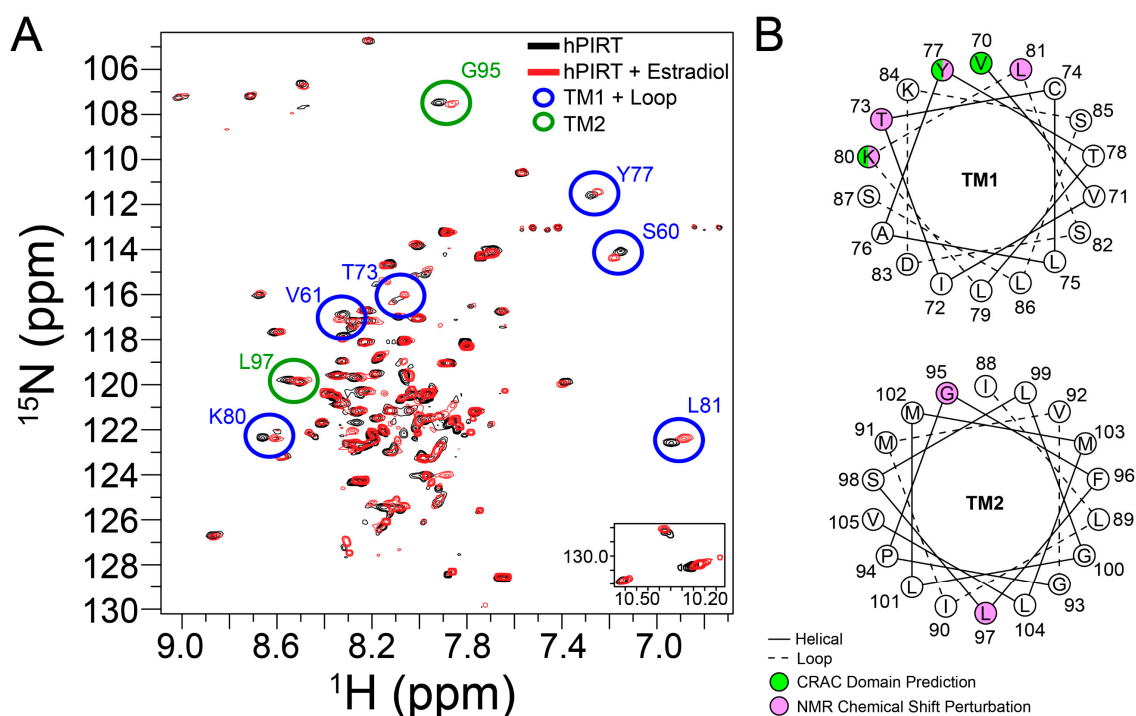


Figure 5. Identification of the PIRT- β -estradiol binding site by NMR. (A) The NMR HSQC of PIRT (black) overlaid against PIRT with a 3.82-mole percent β -estradiol (red). Chemical shift perturbations are seen in the first transmembrane α -helix (S60, V61, T73, Y77, K80, and L81) and second transmembrane α -helix (G95 and L97). (B) Helical wheel projection of the first and second transmembrane α -helices (TM1 and TM2, respectively) with the predicted CRAC domain (green) compared to the NMR chemical shift perturbation (pink). The chemical shift perturbation seen in the upper sections of the α -helices supports the CRAC domain prediction. Residues S60 and V61 in TM1 and G95 and L97 in TM2 suggest there might be a conformational change when β -estradiol binds with PIRT.

3.8. Microscale Thermophoresis Shows PIRT Binds to Other Trp Channel Modulators

Cholecalciferol, the pro-hormone form of vitamin-D synthesized in the skin, has low structural similarity to cholesterol-like molecules but is known to affect TRPV6 [52]. The MST data show that PIRT specifically interacts, albeit with low affinity, to this secosteroid with an apparent $K_d = 2.1 \pm 0.4$ mM (Figure S7). Similarly, PIRT affects oxytocin-induced uterine contraction pain in a TRPV1-dependent manner [14], which we used to test the hypothesis that PIRT may bind to oxytocin. Remarkably, PIRT binds to oxytocin with a $K_d = 7 \pm 1$ μ M (Figure S7), and yet it does not bind to the structurally similar peptide hormone R8-arginine vasopressin (Figure S3C).

To show the significance of the MST binding data, we used nicotinamide (Figure S3D) as a control because it has well-known metabolism and should not interact with PIRT. In previous MST PIRT binding studies using similar conditions, DMSO was previously shown to not bind to PIRT [24].

4. Discussion

Regulation of TRP channels by PIP_2 , Ca^{2+} , and CaM is an active area of research. Several reviews highlight the important features of these TRP channel modulatory mechanisms [53–57]. For some TRPV channels, it is clear that CaM directly binds these channels and regulates function [58,59]. Structural studies of TRPV5 indicate that a single CaM can bridge two distinct TRPV5 binding sites [58]. Similarly, TRPV1 has at least two CaM binding sites, one in the N-terminal ankyrin repeat domain (ARD) and another in the distal C-terminus (CT) [59]. The ARD CaM-binding site functions in desensitization, while the CT CaM interaction has a higher affinity (lower K_d), it has a less defined functional consequence [59]. Titration of holo-CaM to the isolated TRPV1 distal C-terminus (CT) as monitored by tryptophan fluorescence emission identifies an affinity of $K_d = 5.4 \times 10^{-8}$ M [59] which is on par with the affinities identified between PIRT and CaM in this study. However, one significant distinction is that PIRT has a higher affinity for apo-CaM; whereas, it is generally thought that holo-CaM, the Ca^{2+} -bound form, is the regulatory form that plays a role in TRP channel desensitization [55]. While CaM modulation can be direct (i.e., direct binding to TRP channels), modulation can also happen indirectly by impacting other TRP regulatory proteins such as CaM-dependent regulation of phosphatases or kinases [16]. In TRPM8, CaM has been clearly shown to downregulate function indirectly [16]. There is also some evidence that CaM directly binds to TRPM8 [60,61], which would provide an additional mechanism of CaM-mediated functional downregulation. Beyond Ca^{2+} -CaM modulation, at least for TRPM8 and other TRPM channels, it is clear that Ca^{2+} can directly bind and desensitize these channels in the absence of CaM [62]. Our PIRT studies identify a CaM-binding site that adds an additional layer of complexity to TRP channel function and modulation, where PIRT could impact both direct and indirect CaM regulatory functions.

Using purified full-length human PIRT, we show it binds to CaM at the predicted C-terminal α -helix, which suggests a possible role in regulating TRP channel function in concert with calcium and PIP_2 and suggests a broader modulatory role in ion channel regulation. With MST, calcium bound CaM showed an approximately 200 \times decrease in affinity for PIRT than for the apo (calcium unbound) form, which likely arises from known CaM conformational changes upon calcium loading and suggests that calcium-binding of CaM may induce the dissociation of the PIRT–CaM interaction (Figure 2). The PIRT–CaM interaction is confirmed with a pull-down experiment showing that CaM co-eluted with PIRT elution.

We further tested PIRT binding to CaM with NMR titrations to provide amino acids specific details and validate our theoretical CaM binding site on PIRT. Using our previously published PIRT amino acid resonance assignments [24], we show that calcium-free CaM binds to PIRT in the predicted C-terminal α -helix and that the changes in chemical shift indeed correspond to the predicted CaM-binding motif (Figure 1C). The CaM-dependent chemical shift perturbations show several amino acids that display binding, highlighting a possible allosteric effect arising from the interaction. To model our biochemical and biophysical measurements, we used the chemical shift assignments to make Rosetta fragments allowing us to computationally model CaM bound to the PIRT C-terminal α -helix. Our docked

model shows that the C-terminal α -helix fits well within the conserved CaM-binding motif with the hydrophobic Ile113 fitting in the C-terminal lobe and Leu127 in the N-terminal lobe of CaM from PDB entry 2K0F (Figure 1).

Apo-CaM binding to PIRT can be used to expand on known CaM downregulation of the TRPM8 function [16]. Cryo-EM structures of TRPM8 show that Ca^{2+} binds to the human TRPM8 S1-S4 membrane domain with Ca^{2+} chelated by Glu782, Gln785, Tyr793, Asn799, and Asp802 to prime the channel for activation [34,62]. These amino acids, as well as Glu1068, are conserved for all Ca^{2+} dependent TRPM channels (TRPM2, M4, M5, and M8) [15,63–65]. This conservation for Ca^{2+} dependent TRP channels, and their structural homology, suggest that TRPM8 potentially binds to Ca^{2+} in the same location and potentially has a similar effect on the channel. In TRPM8 channels, especially, elevated levels of intracellular Ca^{2+} causes CaM downregulation of TRPM8 with a mechanism that depends on PIP_2 [16]. We previously showed that PIRT reduces the human TRPM8-dependent currents by binding directly to the human TRPM8 S1-S4 domain [23] and shuttles PIP_2 to TRPM8 [24], and this mechanism is plausible for PIP_2 specific inactivation of TRPM8. The data presented here support a more complex mechanism that contextualizes CaM, PIP_2 , Ca^{2+} , and PIRT downregulation of TRPM8 dependent currents.

Figure 6 contextualizes the known interactions that have been identified and relate CaM, Ca^{2+} , PIRT, and PIP_2 to TRPM8 modulation. TRPM8 integrates a variety of stimuli, including, but not limited to, temperature, menthol, and pH. These inputs are then modulated by an additional layer of interactions between PIRT, CaM, and PIP_2 , where PIRT can bind to apo-CaM and PIP_2 , thereby modulating TRPM8 access to these modulators. Currently, the regulatory cross-talk between CaM and PIP_2 is unknown, but given the spatial locations and apparent overlap of the respective PIRT binding sites, it likely impacts the regulatory network. TRPM8 gating by its canonical stimuli (i.e., cold) is thereby further tuned by a variety of modulators, including PIRT, that will ultimately regulate calcium influx and thereby initiating signal transduction. Increases in intracellular calcium concentrations result in direct Ca^{2+} -dependent TRPM8 desensitization [62]. Increased available calcium will also impact CaM leading to higher concentrations of holo-CaM. As a result, because of the decreased affinity of the PIRT—holo-CaM complex, we speculate that the complex would dissociate. Once the calcium levels return to equilibrium, then the PIRT—CaM interaction cycle would continue with apo-CaM rebinding PIRT. The apo-CaM and PIRT complex could potentially allow the channel to become active again by allowing PIP_2 to be shuttled to TRPM8 when the complex is formed. More studies that test the intricacies of these putative interactions are still needed, but our data support a more detailed negative regulation from Ca^{2+} for TRPM8-dependent currents.

PIRT appears to regulate function via diverse means. In this vein, we identified a conserved cholesterol-binding domain called CRAC [40] in the first transmembrane α -helix of PIRT, and we show that it does indeed bind to several cholesterol-like molecules with potential implication in ion channel regulation [66]. We chose these ligands based on bioinformatics predictions on the PIRT sequence matching cholesterol-binding motifs as well as ligands implicated in uterine contraction pain (oxytocin and β -estradiol) and a pro-hormone form of vitamin D with ties to TRPV6 (cholecalciferol) [67]. Our data is the first to show that PIRT binds to cholesterol-like molecules with specificity for cholesteryl-hemisuccinate, cortisol, and β -estradiol; however, it does not specifically bind testosterone. Its interaction with cortisol suggests that it may play a more intimate role in TRP channel-specific stress-induced inflammatory processes.

Binding to cholesteryl-hemisuccinate supports cellular electrophysiology measurements where PIRT was shown to interact with the TRPM8 pore domain [23], and it is known that TRPM8 interacts with cholesterol to partition it into cholesterol-rich membrane domains [68]. Additionally, TRPA1 also has a CRAC domain, which affects both membrane partitioning and function [69]. Furthermore, cholesteryl-hemisuccinate was bound in cryo-EM structures of a handful of TRP channels, including TRPC4, TRPM4, TRPV3, and TRPM8 [62,63,70,71]. With this physiological and structural data, and

our cholesterol-binding data and bioinformatics, we have uncovered another layer of PIRT regulation that may implicate it in is much more diverse physiology than previously thought.

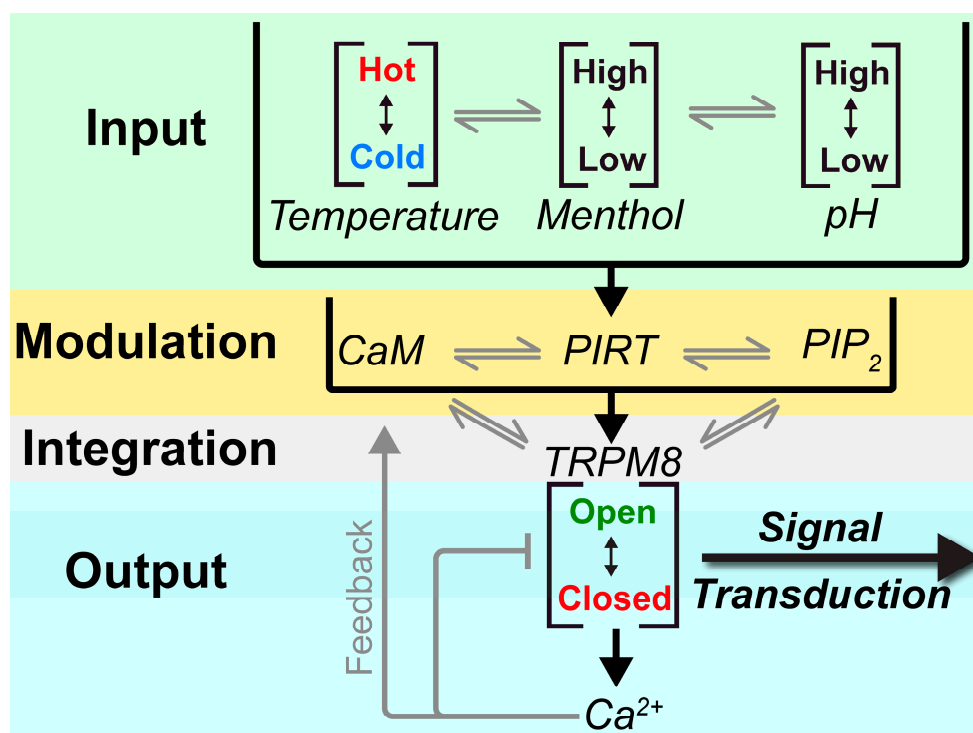


Figure 6. A diagram relating the interactions known so far between CaM, PIRT, PIP₂, TRPM8, and Ca²⁺. Inputs are taken and are modulated by the interactions between CaM, with PIRT and PIRT with PIP₂. These interactions are then integrated to TRPM8, where the channel responds by either opening or closing. Once the channels open, calcium influx occurs, causing signal transduction, and the influx of calcium causes a feedback loop where calcium will bind CaM while also sending negative feedback to TRPM8 and desensitize it.

Interestingly, while β -estradiol (female sex hormone) binds tightly to PIRT, testosterone (male sex hormone) shows no evidence of binding (Figure S3B). This suggests that there may be a sex-specific regulatory role in which PIRT plays a part and may partially explain the role PIRT plays in uterine contraction pain [14]. In addition to uterine contraction pain, TRP channels have been implicated to play a role in cancer cells where expression of these channels can affect cancer cell proliferation, metastasis, and even cell death [72]. In breast cancer cells, the TRPV family and TRPM8 channels expression are regulated by β -estradiol and estrogen receptors [73,74]. Our MST and NMR data show that PIRT binds tightly to β -estradiol and induce some evidence of conformational change in the HSQC, which suggests PIRT might play a role between TRP channels with β -estradiol in breast cancer cells. Supporting the role of PIRT in sex-dependent function, a recent study of PIRT knock-out (^{-/-}) mice indicate that there are subtle PIRT-dependent impacts in metabolism and obesity that are female-specific [75].

Our ligand screen shows that PIRT binding is not limited to cholesterol-like hormones and that cholecalciferol (Vitamin D3) specifically interacts with PIRT. Cholecalciferol is a hormone synthesized in the skin from a cholesterol derivative but is structurally distinct from cholesterol with the sterol backbone disrupted from UV radiation provided by the sun. Vitamin D3 is well known to be intimately involved in bone formation, with recent research on dietary calcium and vitamin D3 being shown to regulate the epithelial ion channels TRPV5 and TRPV6 [67]. It is unknown what role PIRT would directly have on TRPV6 and TRPV5; however, based on emerging evidence of PIRT as a general TRP

channel regulator, it is plausible that PIRT regulates TRPV5 and TRPV6 in concert with the calcium sensor CaM.

Lastly, our studies indicate that PIRT interacts specifically with peptide hormones. We show that PIRT specifically binds oxytocin. It is plausible that PIRT is involved with oxytocin regulation given that the oxytocin receptor is a $G_{q\alpha}$ type G protein-coupled receptor (GPCR), $G_{q\alpha}$ GPCRs directly influence PIP_2 levels, GPCRs are implicated with TRP channels, and PIRT is a PIP_2 binding protein that functionally modulates TRP channels [12–14,23,25,76–78]. Similarly, PIRT was shown to be important for uterine contraction pain under oxytocin insult during birth in mice [14]. Interestingly, while PIRT specifically interacts with oxytocin, it does not bind R8-arginine vasopressin, despite only two amino acid differences in the structurally similar cyclic nonapeptides. It is notable that these hormones have drastically distinct roles in endocrinology, controlling birth induction and blood pressure regulation, respectively. In fact, oxytocin-induced childbirth can result in off-target effects complicating childbirth that are thought to be caused by the similarity of these hormone structures [79,80]. These effects are not fully understood, but with the identification of PIRT, specifically interacting with these hormones, potentially new avenues to understand these side effects can be investigated.

5. Conclusions

The data presented here show several binding partners for PIRT with specific endocrinology roles as well as implicate an enhanced model for TRPM8 regulation. These are the first data to suggest PIRT interactions beyond those with TRP channels and PIP_2 , which opens up multiple avenues of PIRT-related research.

Supplementary Materials: The following are available online at <http://www.mdpi.com/2218-273X/10/3/478/s1>, Figure S1: Characterization of Purified Calmodulin, Figure S2: Representative microscale thermophoresis trace data with PIRT, Figure S3: PIRT Ligand-independent thermophoresis, Figure S4: PIRT conservation across mammalian species, Figure S5: Unguided Rosetta ab initio flexible peptide docking, Figure S6: PIRT and calmodulin pull-down Coomassie-stained gel, Figure S7: PIRT ligand-dependent thermophoresis. A representative coordinate file from the Rosetta modeling of the calmodulin–PIRT interaction.

Author Contributions: Conceptualization, W.D.V.H and N.J.S.; investigation, N.J.S., D.D.L., M.K., and W.D.V.H.; writing—original draft preparation, N.J.S., D.D.L., and W.D.V.H.; writing—review and editing, N.J.S., D.D.L., M.K., and W.D.V.H.; visualization, N.J.S., D.D.L., and W.D.V.H.; funding acquisition, W.D.V.H. All authors have read and agreed to the published version of the manuscript.

Funding: This research was funded by the National Institutes of General Medical Sciences, grant number R01GM112077 (W.D.V.H.).

Acknowledgments: We acknowledge the generosity of Professors Walter Chazin (Vanderbilt University School of Medicine) and Jeremy Mills (Arizona State University) for their material and intellectual support in expression and purification of human calmodulin.

Conflicts of Interest: The authors declare no conflict of interest.

References

1. Veldhuis, N.A.; Poole, D.P.; Grace, M.; McIntyre, P.; Bunnett, N.W. The G protein-coupled receptor-transient receptor potential channel axis: Molecular insights for targeting disorders of sensation and inflammation. *Pharmacol. Rev.* **2015**, *67*, 36–73. [[CrossRef](#)] [[PubMed](#)]
2. Proudfoot, C.J.; Garry, E.M.; Cottrell, D.F.; Rosie, R.; Anderson, H.; Robertson, D.C.; Fleetwood-Walker, S.M.; Mitchell, R. Analgesia mediated by the TRPM8 cold receptor in chronic neuropathic pain. *Curr. Biol.* **2006**, *16*, 1591–1605. [[CrossRef](#)] [[PubMed](#)]
3. Tsavaler, L.; Shapero, M.H.; Morkowski, S.; Laus, R. Trp-p8, a novel prostate-specific gene, is up-regulated in prostate cancer and other malignancies and shares high homology with transient receptor potential calcium channel proteins. *Cancer Res.* **2001**, *61*, 3760–3769. [[PubMed](#)]
4. Zhang, L.; Barritt, G.J. Evidence that TRPM8 is an androgen-dependent Ca^{2+} channel required for the survival of prostate cancer cells. *Cancer Res.* **2004**, *64*, 8365–8373. [[CrossRef](#)] [[PubMed](#)]

5. Ma, S.; Yu, H.; Zhao, Z.; Luo, Z.; Chen, J.; Ni, Y.; Jin, R.; Ma, L.; Wang, P.; Zhu, Z.; et al. Activation of the cold-sensing TRPM8 channel triggers UCP1-dependent thermogenesis and prevents obesity. *J. Mol. Cell Biol.* **2012**, *4*, 88–96. [[CrossRef](#)] [[PubMed](#)]
6. Rossi, H.L.; Jenkins, A.C.; Kaufman, J.; Bhattacharyya, I.; Caudle, R.M.; Neubert, J.K. Characterization of bilateral trigeminal constriction injury using an operant facial pain assay. *Neuroscience* **2012**, *224*, 294–306. [[CrossRef](#)]
7. Tominaga, M.; Caterina, M.J.; Malmberg, A.B.; Rosen, T.A.; Gilbert, H.; Skinner, K.; Raumann, B.E.; Basbaum, A.I.; Julius, D. The cloned capsaicin receptor integrates multiple pain-producing stimuli. *Neuron* **1998**, *21*, 531–543. [[CrossRef](#)]
8. Garami, A.; Shimansky, Y.P.; Rumbus, Z.; Vizin, R.C.L.; Farkas, N.; Hegyi, J.; Szakacs, Z.; Solymar, M.; Csenkey, A.; Chiche, D.A.; et al. Hyperthermia induced by transient receptor potential vanilloid-1 (TRPV1) antagonists in human clinical trials: Insights from mathematical modeling and meta-analysis. *Pharmacol. Tarmacol.* **2020**, *1*, 107474. [[CrossRef](#)]
9. Koplak, P.A.; Rosenberg, R.L.; Oxford, G.S. The role of calcium in the desensitization of capsaicin responses in rat dorsal root ganglion neurons. *J. Neurosci. Res.* **1997**, *17*, 3525–3537. [[CrossRef](#)]
10. Hetenyi, A.; Nemeth, L.; Weber, E.; Szakonyi, G.; Winter, Z.; Josvay, K.; Bartus, E.; Olah, Z.; Martinek, T.A. Competitive inhibition of TRPV1-calmodulin interaction by vanilloids. *FEBS Lett.* **2016**, *590*, 2768–2775. [[CrossRef](#)]
11. Grycova, L.; Holendova, B.; Lansky, Z.; Bumba, L.; Jirku, M.; Bousova, K.; Teisinger, J. Ca²⁺ binding protein S100A1 competes with calmodulin and PIP₂ for binding site on the C-terminus of the TRPV1 receptor. *ACS Chem. Neurosci.* **2015**, *6*, 386–392. [[CrossRef](#)]
12. Kim, A.Y.; Tang, Z.; Liu, Q.; Patel, K.N.; Maag, D.; Geng, Y.; Dong, X. Pirt, a phosphoinositide-binding protein, functions as a regulatory subunit of TRPV1. *Cell* **2008**, *133*, 475–485. [[CrossRef](#)]
13. Patel, K.N.; Liu, Q.; Meeker, S.; Udem, B.J.; Dong, X. Pirt, a TRPV1 modulator, is required for histamine-dependent and -independent itch. *PLoS ONE* **2011**, *6*, e20559. [[CrossRef](#)]
14. Wang, C.; Wang, Z.; Yang, Y.; Zhu, C.; Wu, G.; Yu, G.; Jian, T.; Yang, N.; Shi, H.; Tang, M.; et al. Pirt contributes to uterine contraction-induced pain in mice. *Mol. Pain* **2015**, *11*, 57. [[CrossRef](#)]
15. McKemy, D.D.; Neuhauser, W.M.; Julius, D. Identification of a cold receptor reveals a general role for TRP channels in thermosensation. *Nature* **2002**, *416*, 52–58. [[CrossRef](#)]
16. Sarria, I.; Ling, J.; Zhu, M.X.; Gu, J.G. TRPM8 acute desensitization is mediated by calmodulin and requires PIP₂: Distinction from tachyphylaxis. *J. Neurophysiol.* **2011**, *106*, 3056–3066. [[CrossRef](#)]
17. Halling, D.B.; Liebeskind, B.J.; Hall, A.W.; Aldrich, R.W. Conserved properties of individual Ca²⁺-binding sites in calmodulin. *Proc. Natl. Acad. Sci. USA* **2016**, *113*, E1216–E1225. [[CrossRef](#)]
18. Singh, A.K.; McGoldrick, L.L.; Twomey, E.C.; Sobolevsky, A.I. Mechanism of calmodulin inactivation of the calcium-selective TRP channel TRPV6. *Sci. Adv.* **2018**, *4*, eaau6088. [[CrossRef](#)]
19. Kovalevskaya, N.V.; van de Waterbeemd, M.; Bokhovchuk, F.M.; Bate, N.; Bindels, R.J.; Hoenderop, J.G.; Vuister, G.W. Structural analysis of calmodulin binding to ion channels demonstrates the role of its plasticity in regulation. *Pflugers Arch.* **2013**, *465*, 1507–1519. [[CrossRef](#)]
20. Han, B.; He, K.; Cai, C.; Tang, Y.; Yang, L.; Heinemann, S.H.; Hoshi, T.; Hou, S. Human EAG channels are directly modulated by PIP₂ as revealed by electrophysiological and optical interference investigations. *Sci. Rep.* **2016**, *6*, 23417. [[CrossRef](#)]
21. Sun, J.; MacKinnon, R. Cryo-EM structure of a KCNQ1/CaM complex reveals insights into congenital long QT syndrome. *Cell* **2017**, *169*, 1042–1050. [[CrossRef](#)] [[PubMed](#)]
22. Rohacs, T.; Lopes, C.M.; Michailidis, I.; Logothetis, D.E. PI(4,5)P₂ regulates the activation and desensitization of TRPM8 channels through the TRP domain. *Nat. Neurosci.* **2005**, *8*, 626–634. [[CrossRef](#)] [[PubMed](#)]
23. Hilton, J.K.; Salehpour, T.; Sisco, N.J.; Rath, P.; Van Horn, W.D. Phosphoinositide-interacting regulator of TRP (PIRT) has opposing effects on human and mouse TRPM8 ion channels. *J. Biol. Chem.* **2018**, *293*, 9423–9434. [[CrossRef](#)] [[PubMed](#)]
24. Sisco, N.J.; Helsell, C.V.M.; Van Horn, W.D. Competitive interactions between PIRT, the cold sensing ion channel TRPM8, and PIP₂ suggest a mechanism for regulation. *Sci. Rep.* **2019**, *9*, 14128. [[CrossRef](#)] [[PubMed](#)]
25. Wang, C.; Gu, L.; Ruan, Y.; Gegen, T.; Yu, L.; Zhu, C.; Yang, Y.; Zhou, Y.; Yu, G.; Tang, Z. Pirt together with TRPV1 is involved in the regulation of neuropathic pain. *Neural Plast.* **2018**, *2018*, 4861491. [[CrossRef](#)] [[PubMed](#)]

26. Gao, X.F.; Feng, J.F.; Wang, W.; Xiang, Z.H.; Liu, X.J.; Zhu, C.; Tang, Z.X.; Dong, X.Z.; He, C. Pirt reduces bladder overactivity by inhibiting purinergic receptor $P2 \times 3$. *Nat. Commun.* **2015**, *6*, 7650. [[CrossRef](#)]
27. Guo, W.; Sui, Q.Q.; Gao, X.F.; Feng, J.F.; Zhu, J.; He, C.; Knight, G.E.; Burnstock, G.; Xiang, Z. Co-localization of Pirt protein and $P2 \times 2$ receptors in the mouse enteric nervous system. *Purinergic Signal.* **2016**, *12*, 489–496. [[CrossRef](#)]
28. Sun, J.; MacKinnon, R. Structural basis of human KCNQ1 modulation and gating. *Cell* **2020**, *180*, 340–347. [[CrossRef](#)]
29. Cao, C.; Zakharian, E.; Borbiri, I.; Rohacs, T. Interplay between calmodulin and phosphatidylinositol 4,5-bisphosphate in Ca^{2+} -induced inactivation of transient receptor potential vanilloid 6 channels. *J. Biol. Chem.* **2013**, *288*, 5278–5290. [[CrossRef](#)]
30. Ziemba, B.P.; Swisher, G.H.; Masson, G.; Burke, J.E.; Williams, R.L.; Falke, J.J. Regulation of a coupled MARCKS-PI3K lipid kinase circuit by calmodulin: Single-molecule analysis of a membrane-bound signaling module. *Biochemistry* **2016**, *55*, 6395–6405. [[CrossRef](#)]
31. Brewer, G.J. Calmodulin, zinc, and calcium in cellular and membrane regulation: An interpretive review. *Am. J. Hematol.* **1980**, *8*, 231–248. [[CrossRef](#)]
32. Means, A.R.; Dedman, J.R. Calmodulin—An intracellular calcium receptor. *Nature* **1980**, 73–77. [[CrossRef](#)] [[PubMed](#)]
33. Heizmann, C.W.E. *Calcium-Binding Proteins of the EF-Hand Superfamily from Basics to Medical Applications*; Heizmann, C.W., Ed.; Springer: New York, NY, USA, 2019. [[CrossRef](#)]
34. Yin, Y.; Le, S.C.; Hsu, A.L.; Borgnia, M.J.; Yang, H.; Lee, S.-Y. Structural basis of cooling agent and lipid sensing by the cold-activated TRPM8 channel. *Science* **2019**, 9334, eaav9334. [[CrossRef](#)] [[PubMed](#)]
35. Cao, E.; Cordero-Morales, J.F.; Liu, B.; Qin, F.; Julius, D. TRPV1 channels are intrinsically heat sensitive and negatively regulated by phosphoinositide lipids. *Neuron* **2013**, *77*, 667–679. [[CrossRef](#)] [[PubMed](#)]
36. Collins, M.D.; Gordon, S.E. Short-chain phosphoinositide partitioning into plasma membrane models. *Biophys. J.* **2013**, *105*, 2485–2494. [[CrossRef](#)] [[PubMed](#)]
37. Brauchi, S.; Orta, G.; Mascayano, C.; Salazar, M.; Raddatz, N.; Urbina, H.; Rosenmann, E.; Gonzalez-Nilo, F.; Latorre, R. Dissection of the components for PIP₂ activation and thermosensation in TRP channels. *Proc. Natl. Acad. Sci. USA* **2007**, *104*, 10246–10251. [[CrossRef](#)] [[PubMed](#)]
38. Liu, B.; Qin, F. Functional control of cold- and menthol-sensitive TRPM8 ion channels by phosphatidylinositol 4,5-bisphosphate. *J. Neurosci.* **2005**, *25*, 1674–1681. [[CrossRef](#)]
39. Nelson, M.R.; Chazin, W.J. Structures of EF-hand Ca^{2+} -binding proteins: Diversity in the organization, packing and response to Ca^{2+} binding. *BioMetals* **1998**, *11*, 297–318. [[CrossRef](#)]
40. Fantini, J.; Barrantes, F.J. How cholesterol interacts with membrane proteins: An exploration of cholesterol-binding sites including CRAC, CARC, and tilted domains. *Front. Physiol.* **2013**, *4*, 31. [[CrossRef](#)]
41. Raveh, B.; London, N.; Zimmerman, L.; Schueler-Furman, O. Rosetta FlexPepDock ab-initio: Simultaneous folding, docking and refinement of peptides onto their receptors. *PLoS ONE* **2011**, *6*, e18934. [[CrossRef](#)]
42. Vernon, R.; Shen, Y.; Baker, D.; Lange, O.F. Improved chemical shift based fragment selection for CS-Rosetta using Rosetta3 fragment picker. *J. Biomol. NMR* **2013**, *57*, 117–127. [[CrossRef](#)] [[PubMed](#)]
43. Conway, P.; Tyka, M.D.; DiMaio, F.; Konerding, D.E.; Baker, D. Relaxation of backbone bond geometry improves protein energy landscape modeling. *Protein Sci.* **2014**, *23*, 47–55. [[CrossRef](#)] [[PubMed](#)]
44. Rath, P.; Hilton, J.K.; Sisco, N.J.; Van Horn, W.D. Implications of human transient receptor potential melastatin 8 (TRPM8) channel gating from menthol binding studies of the sensing domain. *Biochemistry* **2016**, *55*, 114–124. [[CrossRef](#)]
45. Wienken, C.J.; Baaske, P.; Rothbauer, U.; Braun, D.; Duhr, S. Protein-binding assays in biological liquids using microscale thermophoresis. *Nat. Commun.* **2010**, *1*, 100. [[CrossRef](#)] [[PubMed](#)]
46. Kim, M.; Sisco, N.J.; Hilton, J.K.; Montano, C.M.; Castro, M.A.; Cherry, B.R.; Levitus, M.; Van Horn, W.D. Evidence that the TRPV1 S1–S4 membrane domain contributes to thermosensing. *bioRxiv* **2019**. [[CrossRef](#)]
47. Delaglio, F.; Grzesiek, S.; Vuister, G.W.; Zhu, G.; Pfeifer, J.; Bax, A. NMRPipe: A multidimensional spectral processing system based on UNIX pipes. *J. Biomol. NMR* **1995**, *6*, 277–293. [[CrossRef](#)]
48. Vranken, W.F.; Boucher, W.; Stevens, T.J.; Fogh, R.H.; Pajon, A.; Llinas, M.; Ulrich, E.L.; Markley, J.L.; Ionides, J.; Laue, E.D. The CCPN data model for NMR spectroscopy: Development of a software pipeline. *Proteins* **2005**, *59*, 687–696. [[CrossRef](#)]

49. Yap, K.L.; Kim, J.; Truong, K.; Sherman, M.; Yuan, T.; Ikura, M. Calmodulin target database. *J. Struct. Funct. Genom.* **2000**, *1*, 8–14. [[CrossRef](#)]
50. White, R.R.; Kwon, Y.-G.; Taing, M.; Lawrence, D.S.; Edelman, A.M. Definition of optimal substrate recognition motifs of Ca²⁺-calmodulin-dependent protein kinases IV and II reveals shared and distinctive features. *J. Biol. Chem.* **1998**, *273*, 3166–3172. [[CrossRef](#)]
51. Rice, P.; Longden, I.; Bleasby, A. EMBOSS: The european molecular biology open software suite. *Trends Genet.* **2000**, *16*, 276–277. [[CrossRef](#)]
52. Walters, J.R.; Balesaria, S.; Chavele, K.M.; Taylor, V.; Berry, J.L.; Khair, U.; Barley, N.F.; van Heel, D.A.; Field, J.; Hayat, J.O.; et al. Calcium channel TRPV6 expression in human duodenum: Different relationships to the vitamin D system and aging in men and women. *J. Bone Miner. Res.* **2006**, *21*, 1770–1777. [[CrossRef](#)] [[PubMed](#)]
53. Rohacs, T. Phosphoinositide Regulation of TRP Channels. *Handb. Exp. Pharmacol.* **2014**, *223*, 1143–1176. [[PubMed](#)]
54. Nilius, B.; Owsianik, G.; Voets, T. Transient receptor potential channels meet phosphoinositides. *EMBO J.* **2008**, *27*, 2809–2816. [[CrossRef](#)]
55. Gordon-Shaag, A.; Zagotta, W.N.; Gordon, S.E. Mechanism of Ca²⁺-dependent desensitization in TRP channels. *Channels* **2008**, *2*, 125–129. [[CrossRef](#)] [[PubMed](#)]
56. Hasan, R.; Zhang, X. Ca²⁺ regulation of TRP ion channels. *Int. J. Mol. Sci.* **2018**, *19*, 1256. [[CrossRef](#)] [[PubMed](#)]
57. Zhu, M.X. Multiple roles of calmodulin and other Ca²⁺-binding proteins in the functional regulation of TRP channels. *Pflugers Arch.* **2005**, *451*, 105–115. [[CrossRef](#)]
58. Hughes, T.E.T.; Pumroy, R.A.; Yazici, A.T.; Kasimova, M.A.; Fluck, E.C.; Huynh, K.W.; Samanta, A.; Molugu, S.K.; Zhou, Z.H.; Carnevale, V.; et al. Structural insights on TRPV5 gating by endogenous modulators. *Nat. Commun.* **2018**, *9*, 4198. [[CrossRef](#)]
59. Lau, S.Y.; Procko, E.; Gaudet, R. Distinct properties of Ca²⁺-calmodulin binding to N- and C-terminal regulatory regions of the TRPV1 channel. *J. Gen. Physiol.* **2012**, *140*, 541–555. [[CrossRef](#)]
60. Qin, N.; Flores, C.M. Polypeptide Complex of TRPM8 and Calmodulin and Its Uses Thereof. U.S. Patent 2007/0105155 A1, 10 May 2007.
61. Hasan, R.; Leeson-Payne, A.T.S.; Jaggar, J.H.; Zhang, X. Calmodulin is responsible for Ca²⁺-dependent regulation of TRPA1 Channels. *Sci. Rep.* **2017**, *7*, 45098. [[CrossRef](#)]
62. Diver, M.M.; Cheng, Y.; Julius, D. Structural insights into TRPM8 inhibition and desensitization. *Science* **2019**, *6672*, eaax6672. [[CrossRef](#)]
63. Autzen, H.E.; Myasnikov, A.G.; Campbell, M.G.; Asarnow, D.; Julius, D.; Cheng, Y. Structure of the human TRPM4 ion channel in a lipid nanodisc. *Science* **2018**, *359*, 228–232. [[CrossRef](#)] [[PubMed](#)]
64. Faouzi, M.; Penner, R. TRPM2. *Handb. Exp. Pharmacol.* **2014**, *222*, 403–426. [[CrossRef](#)] [[PubMed](#)]
65. Hofmann, T.; Chubonov, V.; Gudermann, T.; Montell, C. TRPM5 is a voltage-modulated and Ca²⁺-activated monovalent selective cation channel. *Curr. Biol.* **2003**, *13*, 1153–1158. [[CrossRef](#)]
66. Morales-Lázaro, S.L.; Lemus, L.; Rosenbaum, T. Regulation of thermoTRPs by lipids. *Temperature* **2017**, *4*, 24–40. [[CrossRef](#)]
67. van de Graaf, S.F.; Boullart, I.; Hoenderop, J.G.; Bindels, R.J. Regulation of the epithelial Ca²⁺ channels TRPV5 and TRPV6 by 1 α ,25-dihydroxy Vitamin D3 and dietary Ca²⁺. *J. Steroid Biochem. Mol. Biol.* **2004**, *89–90*, 303–308. [[CrossRef](#)]
68. Morenilla-Palao, C.; Pertusa, M.; Meseguer, V.; Cabedo, H.; Viana, F. Lipid raft segregation modulates TRPM8 channel activity. *J. Biol. Chem.* **2009**, *284*, 9215–9224. [[CrossRef](#)]
69. Startek, J.B.; Boonen, B.; López-Requena, A.; Talavera, A.; Alpizar, Y.A.; Ghosh, D.; Ranst, N.V.; Nilius, B.; Voets, T.; Talavera, K. Mouse TRPA1 function and membrane localization are modulated by direct interactions with cholesterol. *eLife* **2019**, *8*, e46084. [[CrossRef](#)]
70. Huynh, K.W.; Cohen, M.R.; Jiang, J.; Samanta, A.; Lodowski, D.T.; Zhou, Z.H.; Moiseenkova-Bell, V.Y. Structure of the full-length TRPV2 channel by cryo-EM. *Nat. Commun.* **2016**, *7*. [[CrossRef](#)]
71. Duan, J.; Li, J.; Zeng, B.; Chen, G.L.; Peng, X.; Zhang, Y.; Wang, J.; Clapham, D.E.; Li, Z.; Zhang, J. Structure of the mouse TRPC4 ion channel. *Nat. Commun.* **2018**, *9*, 5–14. [[CrossRef](#)]
72. Prevarskaya, N.; Zhang, L.; Barritt, G. TRP channels in cancer. *Biochim. Biophys. Acta Mol. Basis Dis.* **2007**, *1772*, 937–946. [[CrossRef](#)]

73. So, C.L.; Milevskiy, M.J.G.; Monteith, G.R. Transient receptor potential cation channel subfamily V and breast cancer. *Lab. Investig.* **2019**. [[CrossRef](#)] [[PubMed](#)]
74. Chodon, D.; Guilbert, A.; Dhennin-Duthille, I.; Gautier, M.; Telliez, M.-s.; Sevestre, H.; Ouadid-Ahidouch, H. Estrogen regulation of TRPM8 expression in breast cancer cells. *BMC Cancer* **2010**, *10*, 212. [[CrossRef](#)] [[PubMed](#)]
75. Jall, S.; Finan, B.; Collden, G.; Fischer, K.; Dong, X.; Tschöp, M.H.; Müller, T.D.; Clemmensen, C. Pirt deficiency has subtle female-specific effects on energy and glucose metabolism in mice. *Mol. Metab.* **2019**, *23*, 75–81. [[CrossRef](#)] [[PubMed](#)]
76. Hille, B.; Dickson, E.J.; Kruse, M.; Vivas, O.; Suh, B.C. Phosphoinositides regulate ion channels. *Biochim. Biophys. Acta* **2015**, *1851*, 844–856. [[CrossRef](#)] [[PubMed](#)]
77. Tang, Z.; Kim, A.; Masuch, T.; Park, K.; Weng, H.; Wetzel, C.; Dong, X. Pirt functions as an endogenous regulator of TRPM8. *Nat. Commun.* **2013**, *4*, 2179. [[CrossRef](#)] [[PubMed](#)]
78. Tang, M.; Wu, G.Y.; Dong, X.Z.; Tang, Z.X. Phosphoinositide interacting regulator of TRP (Pirt) enhances TRPM8 channel activity in vitro via increasing channel conductance. *Acta Pharmacol. Sin.* **2016**, *37*, 98–104. [[CrossRef](#)]
79. Joo, K.W.; Jeon, U.S.; Kim, G.H.; Park, J.; Oh, Y.K.; Kim, Y.S.; Ahn, C.; Kim, S.; Kim, S.Y.; Lee, J.S.; et al. Antidiuretic action of oxytocin is associated with increased urinary excretion of aquaporin-2. *Nephrol. Dial. Transplant* **2004**, *19*, 2480–2486. [[CrossRef](#)]
80. Sasaki, S. Is oxytocin a player in antidiuresis? *J. Am. Soc. Nephrol.* **2008**, *19*, 189–190. [[CrossRef](#)]



© 2020 by the authors. Licensee MDPI, Basel, Switzerland. This article is an open access article distributed under the terms and conditions of the Creative Commons Attribution (CC BY) license (<http://creativecommons.org/licenses/by/4.0/>).